

## ACCURACY OF 24- AND 48-HOUR FORECASTS OF HAINES' INDEX

Brian E. Potter

USDA Forest Service  
North Central Research Station  
East Lansing, Michigan

Jonathan E. Martin

University of Wisconsin  
Department of Atmospheric and Oceanic Sciences  
Madison, Wisconsin

### Abstract

*The University of Wisconsin-Madison produces Web-accessible, 24- and 48-hour forecasts of the Haines Index (a tool used to measure the atmospheric potential for large wildfire development) for most of North America using its nonhydrostatic modeling system. The authors examined the accuracy of these forecasts using data from 1999 and 2000. Measures used include root-mean-square error (RMSE), mean error (ME), percent misforecast (PM), correlation between error and observed Index value, and Kuiper skill score (K). Average values of these measures indicate that the model forecasts are typically too low (RMSE = 0.74, ME = -0.01 for 24-hour forecasts), about a third (PM=38%) of the point forecasts for the year were misforecast, but that the forecasts are more accurate than random forecasts (K = 0.48). The correlation between error and observed value shows that, in general, the model's predictions are a bit too extreme, pushing the Index values to the ends of the spectrum. Statistics for 48-hour forecasts were similar to those for 24-hour forecasts, indicating that errors arose primarily during the first 24-hours of forecast simulations. Monthly values of the accuracy statistics show winter forecasts to be most accurate and summer forecasts to be least accurate.*

### 1. Introduction

Donald A. Haines (1988) introduced an index for the weather-related aspect of large wildfire risk. Haines referred to this as the Lower Atmospheric Severity Index (LASI), but it has since been renamed the Haines Index (HI) by others, in acknowledgment of Haines' contributions to the science of fire weather. Specifically, the index was intended to indicate the chance that an existing wildland fire would become large and/or erratic in behavior. The Haines Index uses 0000 UTC lower atmospheric stability (lapse rate) and dewpoint depression to produce an integer between 2 and 6 with higher values indicating a dry, unstable atmosphere conducive to the development of large wildfires. This index shows strong ability to distinguish between typical conditions (those under which wildland fires grow slowly and behave somewhat predictably) and rapid fire growth conditions. The HI is currently accepted by many fire weather forecasters and fire managers as a useful tool for evaluating the importance

of atmospheric conditions in fire fighting on a given day.

Brotak (1992-93) concluded that using 1200 UTC sounding data might improve the HI's ability to predict severe fire weather. For documented large fires, HI values of 5 and 6 were more frequent and 2 or 3 values were less frequent in the 1200 UTC data than they were in the 0000 UTC data. Brotak did not determine whether using 1200 UTC data discriminates between extreme fire days and more typical fire days robustly.

Werth and Ochoa (1993) examined the correlation between HI and the daily rate of spread of individual plume dominated fires in Idaho and found a positive correlation between the two quantities. When HI rose, the rate of spread did likewise; when HI fell, so did the rate of spread. They noted that the HI works well for plume-dominated fires, where atmospheric instability plays a strong role. It is not as useful for wind-driven fires, such as those spread by the Santa Ana winds in California, where stability plays less of a role.

Most recently, Werth and Werth (1998) produced a climatology of HI for the Western United States and noted several important findings. Supporting Brotak, they showed that 1200 UTC soundings yield a better measure of synoptic conditions than do 0000 UTC soundings in the western U.S.A. The frequency of HI values of 5 and 6 is notably high over the Great Basin, and notably low over the west coast. The authors observed that the west coast values are for the high-elevation version of the HI, and that perhaps the low or mid-elevation version would be better for lower, coastal areas. In any case, these findings bring into question the ability of HI, or at least the high elevation version, to discriminate between high- and low-risk weather in these regions.

Jones and Maxwell (1998) produced a climatology of HI for New Mexico and examined the use of 1200 UTC versus 0000 UTC measurements. They noted that using 1200 UTC values of HI may underestimate the fire risk, and that perhaps the predicted change from 1200 UTC to 0000 UTC is an important indicator of fire risk.

In 1995, the North Central Research Station (NCRS) of the USDA Forest Service and the Department of Atmospheric and Oceanic Sciences at the University of Wisconsin-Madison began producing 24- and 48-hour computer forecasts of HI and placing them on the Internet World Wide Web. The forecasts continue to provide information to scientists and fire management per-

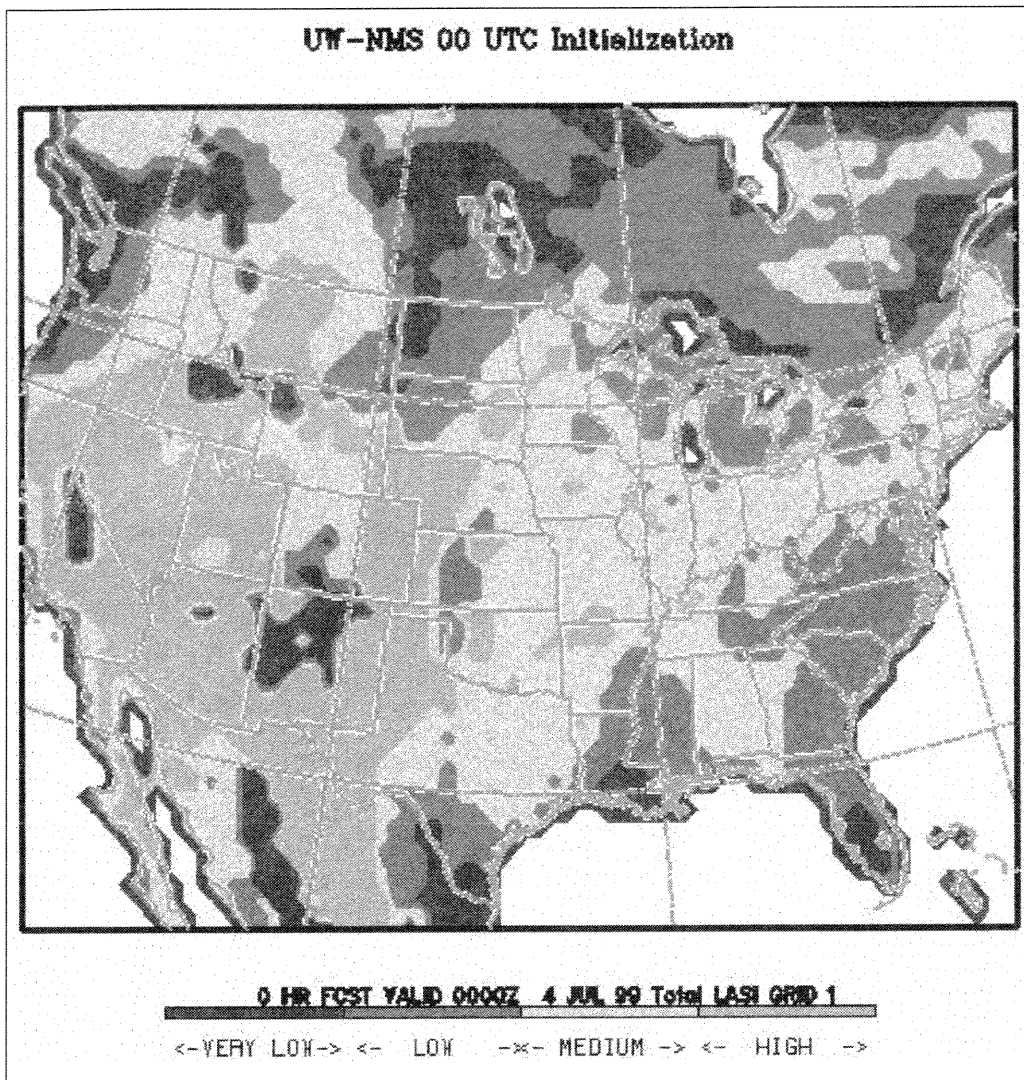


**Fig. 1.** Example of a map of the Haines Index generated by the University of Wisconsin Nonhydrostatic Modeling System. Actual maps are in color.

sonnel at the time of this writing, and are one of a growing number of fire weather forecasts available 48 hours or more in advance.

The current study examines the accuracy of the HI forecasts for 1999 and 2000, the years for which data are most complete. Because there are so few 24- or 48-hour fire weather forecasts available to fire managers and fire forecasters, it is important to assess the HI forecast accuracy as soon as possible. An imperfect measure of forecast accuracy is still an improvement over no measure. Hopefully, a longer-term assessment will be possible in several years, but this two-year assessment is of real value until that time.

## 2. Methods

The University of Wisconsin - Nonhydrostatic Modeling System (UW-NMS) is described by Tripoli (1992a and b). The model employs a two-way interactive, moveable nesting scheme, which allows for the simulta-

neous simulation of large synoptic-scale forcing as well as frontal-scale forcing. Prognostic variables carried by the model include wind ( $u$ ,  $v$ ,  $w$ ), and  $\pi$  (Exner function); ice-liquid potential temperature,  $\theta_{il}$ ; and total water mixing ratio, as well as mixing ratios for a variety of precipitation particles.

Advection of the scalar variables is accomplished using a sixth-order Crowley scheme (Tremback et al. 1987), while the dynamic variables are advected using a second-order enstrophy conserving leapfrog scheme (Sadourny 1975). Model physics include a radiation parameterization that predicts long- and short-wave radiative transfer in a cloudy atmosphere (Chen and Cotton 1983), and a predictive soil model with surface energy budget (Tremback and Kessler 1985). Liquid and ice processes are represented in the model by an explicit microphysics package that describes the evolution of cloud water, rainwater, pristine crystals, snow crystals, aggregate crystals, and graupel (Cotton et al. 1986; Flatau et al. 1989). A version of the Emanuel (1991) convective parameterization is employed, modified such

that the convection equilibrates with the cyclone and frontal-scale vertical motion forcing.

The model employs geometric height as the vertical coordinate with discretely blocked out topography similar to that used in the NOAA/NWS National Centers for Environmental Prediction (NCEP) Eta Model. Forty vertical levels are used with the vertical grid spacing of 200 m in the lowest 5 grid levels with a gradual geometric stretching (by a factor of 1.07) above that, such that the next 18 levels had an average spacing of 404 m, and the top 17 levels have a spacing of 700 m. The model top is located at 19.2 km. For the forecasts used here, the horizontal grid spacing in the model is 60 km.

The model uses the surface elevation at each grid point to determine whether to use the low, middle, or high elevation version of HI. Points below 200 m use the low elevation version, points between 200 m and 1000 m elevation use the middle-elevation version of HI, and points above 1000 m elevation use the high-elevation version. We chose the 200 m and 1000 m thresholds because they

approximate the original regional boundaries from Haines (1988) quite closely.

The model is initialized by interpolating directly from the 90.5-km NCEP Eta initialization, which has 50-mb vertical resolution. Horizontal wind components, geopotential height, temperature, and relative humidity are interpolated horizontally along constant pressure surfaces to the locations of the model grid points. Data are then vertically interpolated to the model grid levels. Finally, the lateral boundaries are updated every 6 h from the Eta gridded forecasts using a Rayleigh-type absorbing layer.

Model initialization maps and 24- and 48-hour forecast maps of the HI were archived throughout 1999 and 2000. Figure 1 shows a typical map, converted to a gray scale. On the maps, the area represented by one pixel varies depending on the latitude of the pixel. At 30°N, one pixel represents an area of 84.7 km<sup>2</sup>, while at 45°N the area is 90.0 km<sup>2</sup>. We made no attempt to adjust the analysis results for this latitude dependence. Map pixel size (roughly 9 km on a side) is not the same as model horizontal resolution (60 km), as the maps were interpolated from the grid. We analyzed the maps because the gridded data are not archived.

Before examining the forecast errors,  $\epsilon$  (predicted value minus observed value), we considered how typical 1999 and 2000 were for fire weather and the HI. We did this in two ways. First, we compared the average area of fires,  $\bar{A}$ , recorded for various regions of the U.S. in 1999 and 2000 (NIFC 2000, 2001) to the 1993-1997 five-year averages for these areas (USDA Forest Service, 1998). While  $\bar{A}$  is strongly affected by human intervention and fire management policies, this provides at least a rudimentary assessment of fire conditions in the two years of interest here.

Our second comparison of the study years with "average" conditions used the UW-NMS initialization maps to determine the average frequency of very low (HI = 2 or 3), low (HI = 4), medium (HI = 5) and high (HI = 6) values of HI for the combined months of June through October. We then compared these frequencies with the results of Werth and Werth (1998) – the nearest thing to a climatology of the Haines Index that is available – for 19 radiosonde stations in the western U.S. The 1999 and 2000 frequencies for a given station were determined as the average of a 5-by-5 pixel box (roughly 45 km on a side) around the actual location of the radiosonde station, not including any geopolitical boundary pixels. (These are colored differently on the maps, and including the pixels in the averaging would have corrupted the results.) The size of the boxes was chosen to reflect our ability to locate the stations on the maps and still include an area that should be thermodynamically uniform.

The verification framework presented by Murphy and Winkler (1987) and the related methods discussed in Murphy and Epstein (1989) and Gandin and Murphy (1992) offer a reasoned, sound basis for model verification. However, due to HI's seasonality and the fact that it is a 4-category index, presentation using Murphy and Winkler's framework would be unmanageably lengthy and complex. We, therefore, present our results using several more conventional and compact measures, bearing in mind their weaknesses as described in the aforemen-

tioned papers. At the end of our monthly analysis, we offer a contingency table for the full two years with a brief discussion of these results.

We present five measures of forecast accuracy, averaging over the entire forecast area and individual months in each case. The mean error (ME) and the root-mean-square error (RMSE) describe the magnitude of the forecast errors. One measure, which we call the percent misforecast (PM), helps determine the frequency in time and space of forecast errors. (The PM is equal to the sum of the off-diagonal elements of the joint probability contingency table.) PM and RMSE are related to one another by the relationship

$$\text{RMSE} = \sqrt{\text{PM}/100} \sqrt{\overline{\text{SE}}} \quad (1)$$

where  $\overline{\text{SE}}$  is the average of the square of all nonzero errors in the forecast. By considering both RMSE and PM, we see whether variations in RMSE stem from the size (SE) or the number (PM) of forecast errors.

The fourth measure we consider is the correlation between monthly mean forecast error and monthly mean observed HI. This correlation provides an indication of whether the forecasts err too high (or low) for high (or low) values of the observed HI.

The last measure we use is the Hanssen-Kuipers discriminant (Hanssen and Kuipers 1965), also known as the Kuiper skill score,  $K$  (Wilks 1995). This uses the observed frequency of HI to assess whether model forecasts are better or worse than random values derived from the observed frequency distribution. A negative  $K$  indicates that the model is worse than the random model,  $K = 0$  means the model is as good as random, and  $K = 1$  means the model always makes perfect forecasts. Based on the definition given in Gandin and Murphy (1992),  $K$  is an equitable skill score (Wilks 1995).

To compute  $\epsilon$ , we first converted the maps to numerical arrays and assigned the colors on the maps cardinal values of 1 (very low, HI = 2 or 3), 2 (low, HI = 4), 3 (medium, HI = 5), and 4 (high, HI = 6) to simplify subsequent calculations. We will use this 1-to-4 scale in all subsequent discussions, unless otherwise noted. We matched each 24-hour forecast array with the 0-hour forecast (i.e., initialization) on the next day, and each 48-hour forecast array with the 0-hour forecast for 2 days later. The 0-hour array was then subtracted from the forecast array, yielding an array of  $\epsilon$  values for that day.

We computed monthly values of all accuracy measures except  $K$  directly from the full data sample for the month (i.e., we did not first compute daily values and then average over the month.) For  $K$ , we computed and averaged daily values for each month because the observed probability distribution,  $p(o)$ , of the Haines Index is not stationary in time and the use of a monthly composite would have altered the monthly  $K$ .

### 3. Results and Discussion

For the comparison of 1999 and 2000  $\bar{A}$  with the 1993-1997 averages, we converted  $\bar{A}$  to standardized scores for

eight regions of the U.S. The comparison for 1999 was complicated by the format of the available data for that year. NIFC (2000) presents the data on a regional basis with four states (ID, OK, TX, and WY) divided across two regions each. Since 1993-1997 and 2000 data are only available on a whole-state basis, and we could not locate

whole-state data for 1999, the comparison for 1999 is not exact. Nonetheless, it still provides useful information for our purposes.

Table 1 shows the standard scores for  $\bar{A}$  for 1999 and 2000. The list of states in each region reflects the states used for computation of the 1993-1997 averages and for the 2000 data. Overall, the U.S. had somewhat larger fires in both years, more so in 2000 than 1999. In 1999, California and the Great Basin had the largest scores and the Southwest had the lowest score. Based on the score signs, the division of the states in the 1999 data could only have an impact on the sign of the scores for the Great Basin and Rocky Mountain regions. Because the Great Basin score was so high (4.00), though, it is not likely to change sign. In 2000, only California had a negative score, and this was of small magnitude. The Rocky Mountain and Northwest scores were large, but even they were small compared to the Northern Rockies, which was over 8 standard deviations above the five-year mean. Overall, 1999 had larger than average fires to the southwest of the Rocky Mountains, and 2000 had large fires everywhere but California. Both years were years of large fires for the United States as a whole.

Compared with the Werth and Werth (1998) climatology of the western U.S., June-October 1999 was a period

of particularly high HI (Table 2). Every region showed a decrease in days when HI = 2 or 3 and an increase in days when HI = 6. Only one station, Grand Junction, Colorado, showed an increase in the frequency of 2 or 3 days and a decrease in days when HI = 6. It appears that 1999 had more high HI days than the 1990-1995 average in the western U.S, but that this only manifested as more fires in the Great Basin region (Nevada and Utah). The period of June through October of 2000 was close to the Werth and Werth climatology, but still showed relatively few HI = 2 or 3 days and more HI = 6 days. The Great Basin, Rocky Mountain, and Southwest stations, with the exception of Tucson, were all fairly close to Werth and Werth's frequencies. The Northern Rockies, so remarkable in terms of  $\bar{A}$  in Table 1, suggest there was a higher than normal risk of large fires, but the 2000 HI frequencies were quite comparable to the 1999 frequencies.

Figure 2 shows monthly RMSE for the 24-hour and 48-hour forecasts. The 24-hour errors are lowest in the winter months, with a sharp May peak in 1999 and a broader peak in June-July of 2000. Errors for 48-hour forecasts are similar to, but slightly larger than,

**Table 1.** Standard scores for average fire area for 1999 and 2000, based on the 1993-1997 averages.

Geographic region (states)	1999	2000
Northwest (OR, WA)	-0.15	3.35
California	2.04	-0.13
Northern Rockies (ID, MT, ND)	0.31	8.07
Rocky Mountain (CO, KS, NE, SD, WY)	-0.21	4.34
Great Basin (UT, NV)	4.00	1.09
Southwest (AZ, NM)	-1.62	1.99
Eastern (CT, DE, IA, IL, IN, MA, MD, ME, MI, MN, MO, NJ, NY, OH, PA, RI, VT, WV)	-0.31	1.76
Southern (AL, AR, FL, GA, KY, LA, MS, NC, OK, SC, TN, TX, VA)	1.04	1.10
United States	1.16	2.40

**Table 2.** Differences in frequency (%) of HI values between 1999 data and Werth and Werth (1998) average values for 1990-1995, and between 2000 data and average 1990-1995 values. Positive values indicate the 1999 or 2000 frequency exceeded Werth and Werth frequency. All differences are for the period of June through October. The sum of the differences for a station may not be zero due to rounding. Regional groupings correspond to those used in Table 1.

Site	1999				2000			
	2 and 3	4	5	6	2 and 3	4	5	6
<b>Northwest</b>								
Quillayute, WA	-33	5	19	4	-34	7	18	8
Spokane, WA	-76	-11	24	61	-66	-2	27	39
Salem, OR	-40	14	15	8	-18	5	9	3
Medford, OR	-47	1	12	31	-43	-6	23	25
<b>California</b>								
San Diego, CA	-40	-26	26	39	-36	-26	18	44
<b>Northern Rockies</b>								
Great Falls, MT	-73	-10	12	69	-64	9	16	38
Glasgow, MT	-69	2	22	46	-65	6	11	48
Boise, ID	-47	-24	-16	86	6	-6	-3	3
<b>Rocky Mountain</b>								
Grand Junction, CO	4	-1	2	-4	-1	-4	-1	7
Denver, CO	-44	-6	5	44	-2	0	10	-8
Lander, WY	-34	4	11	19	-7	-5	2	10
<b>Great Basin</b>								
Winnemucca, NV	-32	-22	-20	72	6	-3	-5	1
Ely, NV	-6	5	3	-5	6	-4	-1	-2
Desert Rock, NV	-33	-22	-33	88	2	2	-4	0
Salt Lake City, UT	-34	-7	14	27	0	-5	-1	6
<b>Southwest</b>								
Winslow, AZ	-44	-21	-12	77	9	-2	0	-7
Tucson, AZ	-75	-15	-2	91	-74	-10	3	80
Albuquerque, NM	-2	8	-4	-2	1	2	7	-10
<b>Average:</b>	<b>-42</b>	<b>-7.2</b>	<b>4.1</b>	<b>44</b>	<b>-20</b>	<b>-1.9</b>	<b>6.7</b>	<b>15</b>

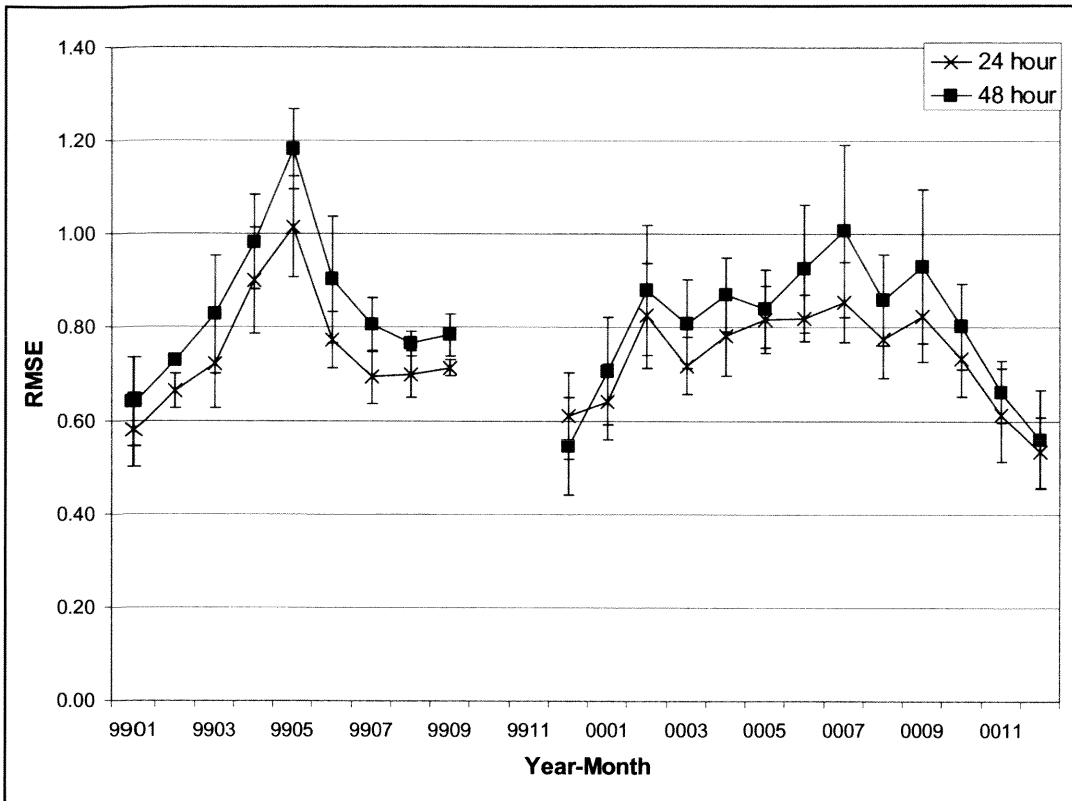


Fig. 2. Monthly root mean square errors (RMSE) for 24-hour and 48-hour forecasts of the Haines Index by the UW-NMS. Error bars indicate one standard deviation in the daily values for any given month.

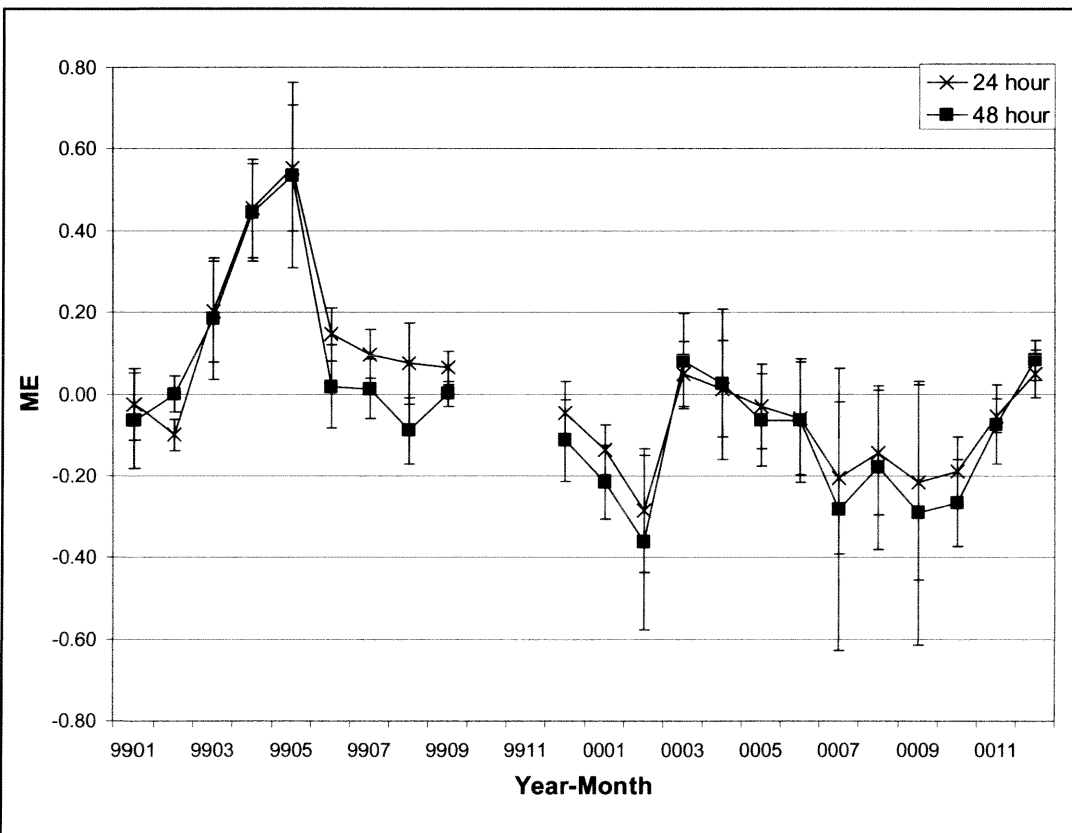


Fig. 3. As in Fig. 2, but showing monthly mean errors (ME).

the 24-hour errors. Both 24- and 48-hour forecasts also had small peaks in February and September of 2000. The highest 24-hour RMSE was 1.0 in May 1999 and the lowest value was 0.5 in December 2000. The 2-year average standard deviation was 0.1; the lowest monthly standard deviation was  $2 \times 10^{-2}$  in September 1999 and the highest was 0.1 in April 1999.

Differences between 24-hour and 48-hour RMSE are about 0.1, comparable to the standard deviation for most months.

Monthly ME values (Fig. 3) were closer to zero in 2000 than in 1999. May 1999 is definitely the month with the largest ME, with April close behind. Overall, the model shows a small positive bias in 1999 (forecast values of HI are too high) and a negative bias in 2000. The 24-hour and 48-hour values of ME are similar in each month.

Monthly PM values appear in Fig. 4. The trends here follow those seen in RMSE (Fig. 2), with summer peaks and winter minima. From equation (1), we determined that the monthly RMSE changes are primarily due to the number of errors, not changes in the magnitude of the errors. The increase in 24-hour PM from 0.24 in January 1999 to 0.51 in May 1999 causes 68% of the increase in RMSE for this period. In essence, the model tends to miss the mark by about the same margin but in May it misses it more often (for more locations

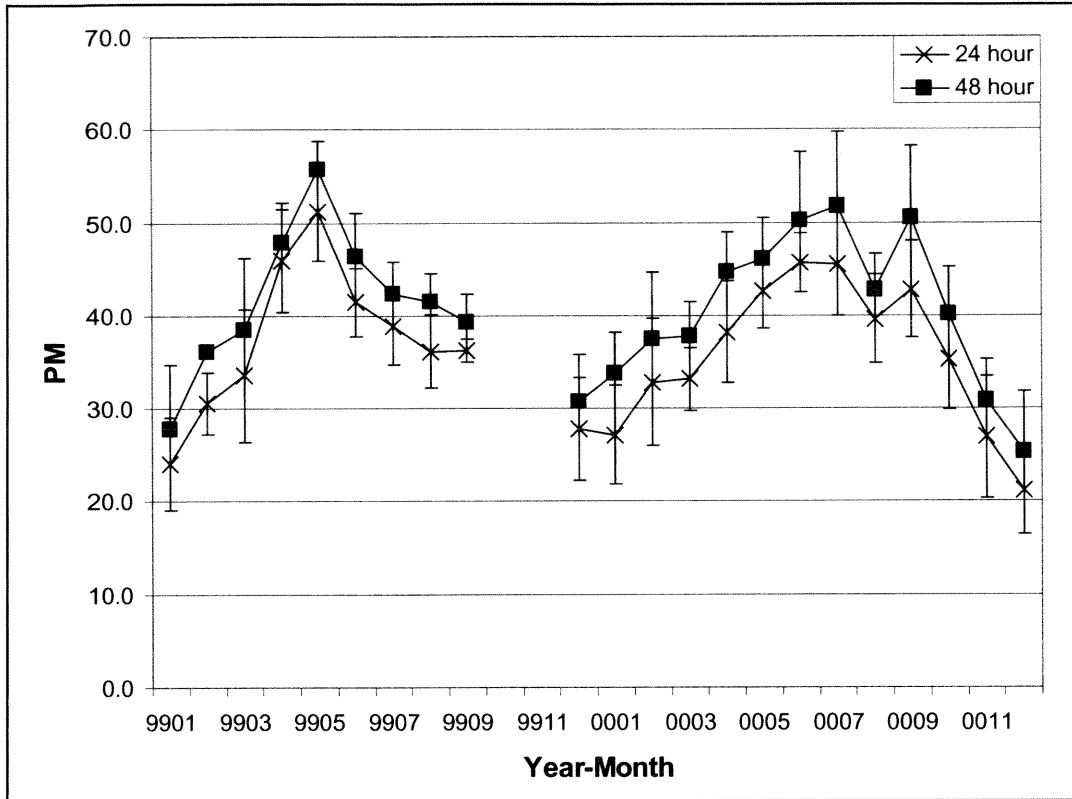


Fig. 4. As in Fig. 2, but showing monthly percent area misforecast (PM).

Table 3. Joint and marginal probability distributions for (a) 24-hour and (b) 48-hour HI forecasts by the UW-NMS.

(a)		Observed HI ( <i>o</i> )				<i>p</i> ( <i>f</i> )
Forecast ( <i>f</i> )	1	2	3	4		
1	0.27	0.04	0.01	0.00	0.32	
2	0.06	0.11	0.04	0.00	0.21	
3	0.02	0.06	0.11	0.03	0.22	
4	0.00	0.02	0.08	0.16	0.26	
<i>p</i> ( <i>o</i> )	0.35	0.23	0.23	0.19		

(b)		Observed HI ( <i>o</i> )				<i>p</i> ( <i>f</i> )
Forecast ( <i>f</i> )	1	2	3	4		
1	0.24	0.05	0.02	0.00	0.31	
2	0.07	0.10	0.05	0.01	0.22	
3	0.02	0.06	0.10	0.03	0.22	
4	0.01	0.03	0.07	0.15	0.26	
<i>p</i> ( <i>o</i> )	0.35	0.23	0.23	0.19		

and on more occasions). The 48-hour PM values are similar to the 24-hour PM values.

Figure 5 is a scatter plot showing the relationship between monthly mean 24-hour forecast error and monthly mean observed HI value. (The distribution using 48-hour forecasts is very similar and not shown.) The distribution suggests that when the HI is low, the model tends to underestimate it and when the HI is high, the

model tends to overestimate it. The correlation coefficient between the errors and observed HI is 0.30, a modest but positive correlation that supports this conclusion. What this means is that the model tends to be a bit extreme: under dry, unstable conditions it predicts conditions that are too wet and/or too unstable, and under moist, stable conditions the model predicts conditions that are too wet and/or too stable.

The monthly Kuiper scores, *K*, are shown in Fig. 6. All scores are positive, meaning that the UW-NMS does better than random at predicting HI. For most months 24-hour *K* is slightly less than 0.5, but in May 1999 it drops to 0.31 and in December 2000 it jumps up to 0.66. The 48-hour *K* is always less

than the 24-hour *K* and greater than zero. In May 1999 it reaches its minimum value of 0.24.

Table 3 shows the joint and marginal probabilities for all days in the 24- and 48-hour data sets (*n*=334 and *n*=284, respectively). There are few large differences between the table entries for the two forecast times, again showing that the longer-lead forecast is only slightly less accurate than the shorter. The probabilities also show that an incorrect forecast is slightly more likely to be too high than too low. The sum of all joint probabilities below the diagonal in the table is the probability of a forecast being too high, and comes to 0.18 for the 24-hour forecasts. The probability of a forecast being too low (i.e., the sum of the probabilities above the diagonal) is 0.14 for the 24-hour forecasts.

#### 4. Conclusions

The five measures of accuracy presented here provide a coherent and consistent picture of UW-NMS's accuracy for forecasting the HI. The model forecasts were more accurate than a random forecast based on the observed probability distribution function, *p*(*o*), but were not perfect, either. When lower atmosphere conditions in the winter were wet and stable, the model overestimated lower atmosphere wetness and stability. The situation was reversed in the summer (already dry, unstable conditions were forecast as drier and more unstable). Throughout the year, with the exception of May, the forecast RMS error was less than 1, meaning the forecast was usually correct and when it missed, it most often missed

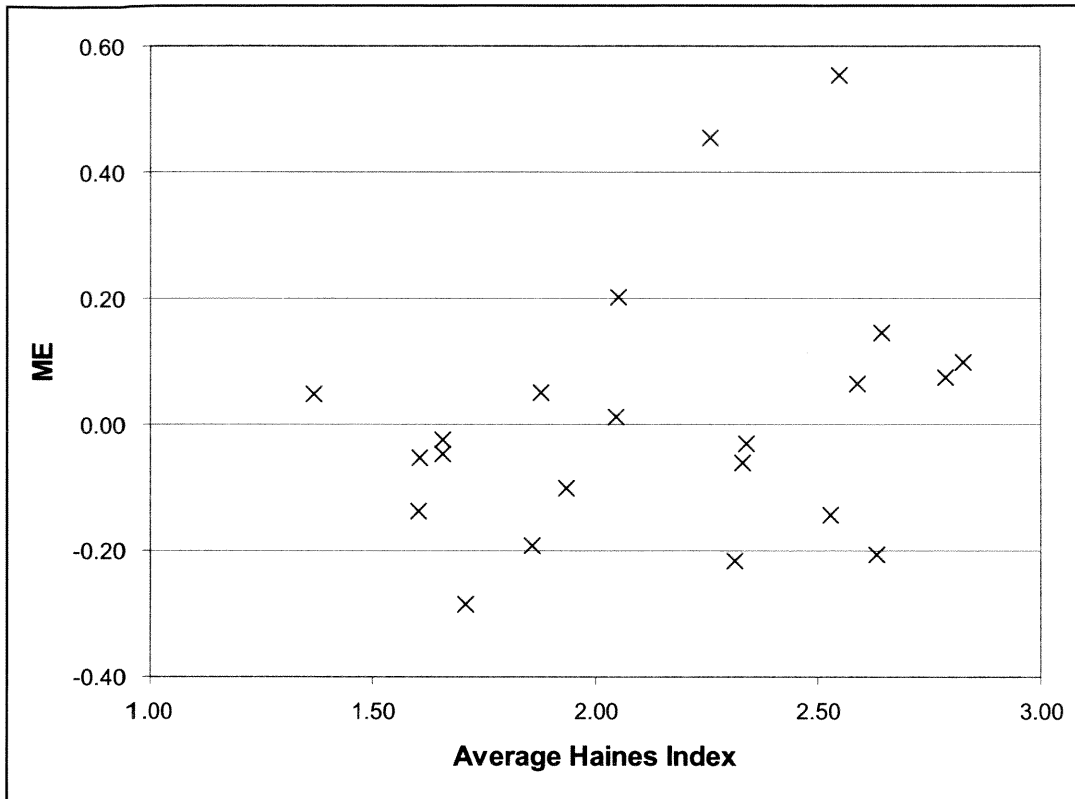


Fig. 5. Scatter plot showing monthly averages of model error (y-axis) against monthly averages of observed Haines Index (x-axis).

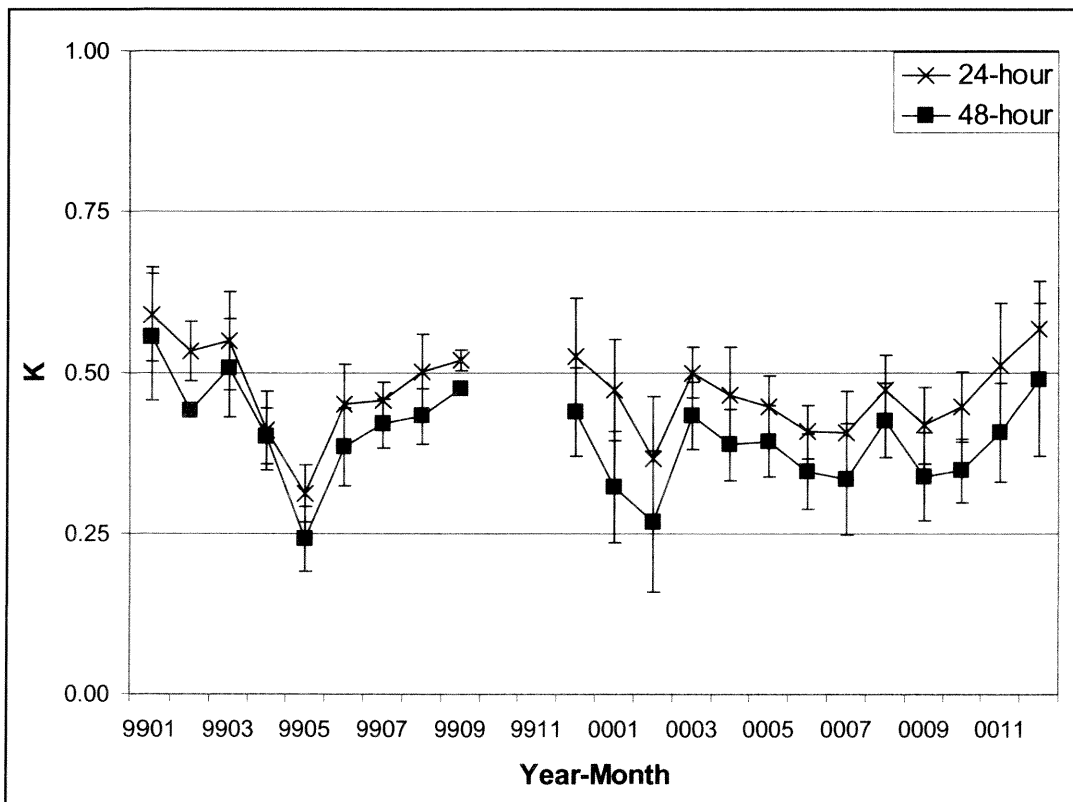


Fig. 6. As in Fig. 2, but showing monthly Kuiper skill scores (K).

by one level (e.g., low or high HI instead of medium HI.) The RMSE increase in April through June 1999 was due more to the number of errors in those months than it was to their magnitude. At this time of year, the model forecast was incorrect about 40 to 50% of the time, roughly 10 percentage points more than at other times of the year. Approximately 90% of the forecast error appeared in the first 24 hours of a forecast simulation, and 48-hour forecasts are only slightly less accurate than the 24-hour forecast.

This study examined the accuracy of UW-NMS forecasts of the HI for 24- and 48-hour lead times in 1999 and 2000. It is an assessment of one model based on two years, and should not be taken as anything more. It does not validate or invalidate any other type of forecast model or method. Nor does it provide any information, other than general qualitative guidance, about the model's accuracy at any other time: the model does better than chance, shows only a slight increase in error from 24- to 48-hours, and seems to be least accurate in the spring.

Most importantly, this study did not examine the accuracy of the Haines Index as a measure of fire risk or fire behavior. It was not a measure of the Index, but of the UW-NMS's ability to forecast the Index accurately.

There are several important questions either left unanswered by this study, or raised by it. We did not exam-

ine spatial patterns in the Index or the forecast errors. These patterns are important, as they may reveal areas of North America where the forecasts are particularly good or bad. These patterns may have seasonal aspects as well. Because fire season varies from one region to another, such patterns and their timing are important properties of the forecast error.

There are alternative ways of forecasting the Haines Index, most notably persistence. (Using climatology is not an option at present, except in the western U.S. where Werth and Werth (1998) analyzed the climatology.) Does the UW-NMS provide any better forecast than persistence? What period of time (1 day, 2 days, etc.) should be used in determining a persistence forecast? Due to the nature of the Index, a persistence forecast based on more than one previous day will require actual lapse rate and dewpoint depression data, something the UW-NMS does not archive.

Finally, as time passes and more forecasts are made with the UW-NMS, the forecast accuracy should be examined for a longer period than one year. There may be overall differences in accuracy, and there will almost certainly be differences in the forecast accuracy within various regions.

### Acknowledgments

The authors thank Mr. Matthew Bromley and Mr. Thor Sawin for their diligent work in computing many of the analysis statistics for the daily forecast maps. The initial work of getting the Haines Index maps onto the World Wide Web was done by Mr. David Westberg under a Research Cost Reimbursement Agreement between the USDA Forest Service and the University of Wisconsin. The comments of the reviewers for NWD were extremely helpful in clarifying portions of the original draft.

### Authors

Dr. Brian Potter is a Research Meteorologist with the USDA Forest Service North Central Research Station in East Lansing, Michigan. In addition to the Haines Index and fire weather, his research interests include the microclimate of forest gaps and the impact silvicultural management techniques on microclimate and regeneration in northern hardwood forests. He obtained his B.A. in Physics from Carleton College in 1986, and his Ph.D. in Atmospheric Sciences from the University of Washington in 1994.

Dr. Jonathan Martin is an Associate Professor of Atmospheric and Oceanic Sciences at the University of Wisconsin at Madison. His main research interests are the structure and evolution of occluded cyclones. He obtained his B.S. in Meteorology and a B.A. in Applied Mathematics from Saint Louis University in 1985 and his Ph.D. in Atmospheric Sciences from the University of Washington in 1992.

### References

Brotak, E. A., 1992-93: Low-level weather conditions preceding major wildfires. *Fire Management Notes*, 53-54, 23-26.

Chen, C., and W. R. Cotton, 1983: A one-dimensional simulation of the stratocumulus capped mixed layer. *Bound.-Layer Meteor.*, 25, 289-321.

Cotton, W. R., G. J. Tripoli, R. M. Rauber and E. A. Mulvihill, 1986: Numerical simulation of the effects of varying ice crystal nucleation rates and aggregation processes on orographic snowfall. *J. Climate Appl. Meteor.*, 25, 1658-1680.

Emanuel, K. A., 1991: A scheme for representing cumulus convection in large-scale models. *J. Atmos. Sci.*, 48, 2313-2335.

Flatua, P., G. J. Tripoli, J. Verlinde, and W. R. Cotton, 1989: The CSU RAMS cloud microphysical module: General theory and code documentation. Tech. Rep. 451, Dept. of Atmos. Sci., Colorado State University, 88 pp. [Available from Dept. of Atmos. Sci., CSU, Fort Collins, CO 80523].

Gandin, L.S. and A.H. Murphy, 1992: Equitable skill scores for categorical forecasts. *Mon. Wea. Rev.*, 120, 361-370.

Haines, D.A., 1988: A lower atmospheric severity index for wildland fires. *Natl. Wea. Dig.*, 13:2, 23-27.

Hanssen, A.W. and W.J.A. Kuipers, 1965: On the relationship between frequency of rain and various meteorological parameters. *Meded. Verh.*, 81, 2-15.

Jones, K.M. and C. Maxwell, 1998: A seasonal Haines Index climatology for New Mexico and the significance of its diurnal variations in the elevated Southwest. Preprints, *Second Conf. on Fire and Forest Meteorology*, Phoenix, Arizona, Amer. Meteor. Soc., 127-130.

Murphy, A.H. and R.L. Winkler, 1987: A general framework for forecast verification. *Mon. Wea. Rev.*, 115, 1330-1338.

\_\_\_\_\_, and E.S. Epstein, 1989: Skill scores and correlation coefficients in model verification. *Mon. Wea. Rev.*, 117, 572-581.

NIFC, 2000: National Fire News. National Interagency Fire Center. As of March 13, 2001, available at <http://www.nifc.gov/fireinfo/1999/nfnmap99.html>.

\_\_\_\_\_, 2001: National Fire News. National Interagency Fire Center. As of March 13, 2001, available at <http://www.nifc.gov/fireinfo/nfnmap.html>.

Sadourny, R., 1975: The dynamics of finite-difference models of the shallow water equations. *J. Atmos. Sci.*, 32, 680-689.

Tremback, C. J., and R. Kessler, 1985: A surface temperature and moisture parameterization for use in mesoscale numerical models. Preprints, *Seventh Conf. on Numerical Weather Prediction*, Montreal, PQ, Canada, Amer. Meteor. Soc., 280-285.



\_\_\_\_\_, J. Powell, W. R. Cotton, and R. A. Pielke, 1987: The forward-in-time upstream advection scheme. Extension to higher orders. *Mon. Wea. Rev.*, 115, 540-555.

Tripoli, G. J., 1992a: An explicit three-dimensional non-hydrostatic numerical simulation of a tropical cyclone. *Meteor. Atmos. Phys.*, 49, 229-254.

\_\_\_\_\_, 1992b: A nonhydrostatic numerical model designed to simulate scale interaction. *Mon. Wea. Rev.*, 120, 1342-1359.

USDA Forest Service, 1998: *1991-1997 Wildland Fire Statistics*. USDA Forest Service, Fire and Aviation Management, 141 pp.

Werth, P., and R. Ochoa 1993: Evaluation of Idaho wild-fire growth using the Haines Index, *Wea. Forecasting*, 8, 223-234.

Werth, J., and P. Werth, 1998: Haines Index climatology for the western United States. *Fire Management Notes*, 58, 8-17.

Wilks, D.S., 1995: *Statistical Methods in the Atmospheric Sciences*, Academic Press, 467 pp.